COPPER-MULTIWALL CARBON NANOTUBES AND COPPER-DIAMOND COMPOSITES FOR ADVANCED ROCKET ENGINES

Biliyar N. Bhat, NASA Marshall Space Flight Center
Dave L. Ellis, NASA Glenn Research Center
Vadim Smelyanskiy and Michael Foygel, Ames Research Center
Aaron Rape and Jogender Singh, Pennsylvania State University
Yogesh K. Vohra and Vinoy Thomas, University of Alabama Birmingham
Kyle G. Otte and Deyu Li, Vanderbilt University

Abstract

This paper reports on the research effort to improve the thermal conductivity of the copper-based alloy NARloy-Z (Cu-3 wt.%Ag-0.5 wt.% Zr), the state-of-the-art alloy used to make combustion chamber liners in regeneratively-cooled liquid rocket engines, using nanotechnology. The approach was to embed high thermal conductivity multiwall carbon nanotubes (MWCNTs) and diamond (D) particles in the NARloy-Z matrix using powder metallurgy techniques. The thermal conductivity of MWCNTs and D have been reported to be 5 to 10 times that of NARloy-Z. Hence, 10 to 20 vol. % MWCNT finely dispersed in NARloy-Z matrix could nearly double the thermal conductivity, provided there is a good thermal bond between MWCNTs and copper matrix. Quantum mechanics-based modeling showed that zirconium (Zr) in NARloy-Z should form ZrC at the MWCNT-Cu interface and provide a good thermal bond. In this study, NARloy-Z powder was blended with MWCNTs in a ball mill, and the resulting mixture was consolidated under high pressure and temperature using Field Assisted Sintering Technology (FAST). Microstructural analysis showed that the MWCNTs, which were provided as tangles of MWCNTs by the manufacturer, did not detangle well during blending and formed clumps at the prior particle boundaries. The composites made form these powders showed lower thermal conductivity than the base NARloy-Z. To eliminate the observed physical agglomeration, tangled multiwall MWCNTs were separated by acid treatment and electroless plated with a thin layer of chromium to keep them separated during further processing. Separately, the thermal conductivities of MWCNTs used in this work were measured, and the results showed very low values, a major factor in the low thermal conductivity of the composite. On the other hand, D particles embedded in NARloy-Z matrix showed much improved thermal conductivity. Elemental analysis showed migration of Zr to the NARloy-Z-D interface to form ZrC, which appeared to provide a low contact thermal resistance. These results are consistent with the quantum mechanics-based model predictions. NARloy-Z-D composites have relatively high thermal conductivities and are promising for further development.

Introduction

Liquid-fueled rocket engine combustion chamber liners are regeneratively cooled to maintain a high heat flux so that the liner surface temperatures are well below the melting point of the liner. NARloy-Z (Cu-3 wt.% Ag-0.5 wt.% Zr alloy) is the state-of-the-art material used to make the liner. The current trend is to develop copper alloys with higher alloy content (e.g., GRCop-84, which contains 8 at.% Cr and 4 at. % Nb) to improve high temperature capability. However, higher alloying results in a lower thermal conductivity (25% lower than Cu for GRCop-84). To alleviate this problem, it was proposed to use multiwall carbon nanotubes (MWCNTs) in a NARloy-Z matrix. The reported thermal conductivities of MWCNTs vary, but can be up to 10X times that of NARloy-Z (Ref. 1). Addition of 10 vol.% of MWCNTs (~2.5% by weight) could nearly double the thermal conductivity of NARloy-Z based upon a rule of mixtures calculation – a huge benefit. The research goal was to increase the thermal conductivity of NARloy-Z by blending MWCNTs with NARloy-Z powder and sintering the blended powder at elevated temperatures to produce a fully dense composite. Advanced high thermal conductivity structural materials produced in this manner will be applicable to components in various propulsion systems, including space transportation, advanced in-space propulsion systems and nuclear propulsion systems. Furthermore, these materials will have many applications in industry, e.g., thermal management for computer hardware, heat exchangers, etc.

A significant effort has gone into using multiwall and single wall carbon nanotubes (CNTs) to improve the thermal conductivity of polymer matrix composites with some success (Ref. 1). The degree of improvement has been modest, however. Improving the thermal conductivity of highly conductive metallic materials using MWCNTs has been more challenging. There are some instances where thermal conductivity has improved somewhat, but nowhere close to the theoretical values. Part of the problem appears to be the contact thermal resistance between the MWCNTs and matrices. The mechanism of thermal conductivity is different in the two components. The thermal conductivity of copper is largely electronic, while CNTs conduct heat along the tube length through phonons (lattice vibrations). It is a challenge to provide a suitable interface between the copper matrix and CNTs that has a low contact thermal resistance. A mixture of copper powder and MWCNTs blended together and sintered at elevated temperature did not show any improvement in thermal conductivity. In fact, the thermal conductivity went down in proportion to the MWCNT content. This result was attributed to poor thermal bonding between MWCNT and copper matrix (Ref. 1, 2)

Improved results were reported when diamond (D), which also transfers heat through phonons, was substituted for MWCNTs. The diamond decreased the thermal conductivity when pure copper powder was used because it acted as scattering sites. On the other hand, copper alloyed with carbide forming elements such as Cr, Zr and Ti provided significant increases in the thermal conductivity of the composites (Ref. 3, 4). While the maximum thermal conductivity of diamond is less than that of CNTs (~1200 W/m-K versus up to 4000 W/m-K reported for CNTs), Cu-D thermal conductivities exceeding that of pure copper were readily obtained. With this background, it was decided to investigate the improvements in thermal conductivities of NARloy-Z-MWCNT composites, correlate them with microstructure, and compare the results with NARloy-Z-D composites.

Analytical Modeling of Kapitza Thermal Resistance

The analytical approach used in this research focused on the MWCNT-copper matrix interface. It was clear from the start that a good thermal bond and a low interface thermal resistance were required. In addition, a good metallurgical bond is needed to impart sufficient mechanical strength to the composite for use in liners and other applications. NARloy-Z was chosen as the matrix material since it contains 0.5% zirconium (Zr). The Zr should diffuse and react with the outermost wall of the MWCNT to form ZrC. ZrC would provide a good thermal and mechanical bond with NARloy-Z.

It is important to develop a good theoretical understanding of the Cu-MWCNT interface through quantum mechanics based modeling, since these interfaces tend to control the thermal properties of these composites. It is necessary to design a high thermal conductivity/low thermal resistance interface. A quantum mechanics-based model for NARloy-Z-MWCNT composite was developed that addressed the

contact thermal conductance (σ) of Cu-CNT interface using a quantum mechanics approach to analyze the Kapitza thermal resistance. The findings are summarized in Figure 1 and Table 1. It is interesting to note that contact conductance is about the same for CNT, graphene and diamond for temperatures (T/θ_m) >1.

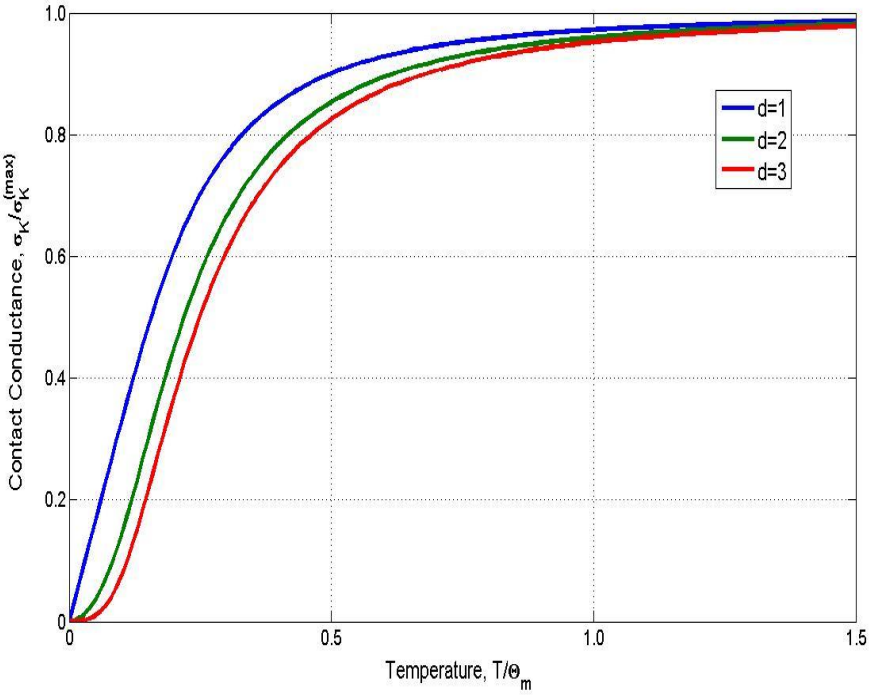

Figure 1: Contact Conductance of Metals with Carbon Modifications: d = 1 (*CNT*), d=2 (graphene, *G*), d = 3 (diamond, *D*). Here θ_m – temperature at maximum phonon frequency (kT = h x frequency where k is Boltzmann's constant and h is Planck's constant) – Debye's temperature is used for θ_m as an approximation.

Table 1: Contact thermal conductance for various interfaces

Parameter / Contact	Θ_m, K	σ^{max}, kW/cm^2K
D/Cu	310	6.6
D/Zr	250	3.5
D/Ag	221	2.4
D/ZrC	680	70
ZrC/Cu	310	35
D/ZrC/Cu	680, 310	23
CNT/Cu	310	$8.9\cdot10^{-13}$, kW/K
G/Cu	310	$2.6\cdot10^{-6}$, $kW/cm\cdot K$

The following observations were made:

1. The D/ZrC/Cu composite is expected to have a contact thermal resistance 3.5 times smaller than that of the direct CNT/Cu contact.
2. D/Zr/Cu or D/Ag/Cu composites may have higher thermal resistance interfaces than the D/Cu interface.

Note: CNT can be used in place of D since they behave in a similar manner as far as contact thermal resistance is concerned. In other words, what works for D should work for CNTs.

The quantum mechanics-based model further shows that:

1. In NARloyZ-CNT composites, the input to the thermal conductivity from the CNTs, whose length exceeds 10 microns, is not likely to be dominated by contact resistance. In other words, longer CNTs should be preferred.
2. Critical CNT length may be reduced by up to 3X if the CNT surfaces are covered with a monolayer of material with Debye's temperature greater than that of copper, such as ZrC or $Cr_{23}C_6$.

These findings were utilized in the experimental approach to develop high thermal conductivity Cu-MWCNT composites.

EXPERIMENTAL PROCEDURE

Table 2 summarizes the compositions studied and the characterization work performed in this study. NARloy-Z powder was blended with MWCNTs in various proportions ranging from 1% to 20% by volume and sintered at elevated temperatures using Field Assisted Sintering Technology (FAST). Blending was done in an attritor at NASA-GRC in an inert nitrogen atmosphere at cryogenic temperatures to prevent oxidation. Sintering was done in a hydrogen atmosphere under high pressure in a carbon die to form fully dense composite. The sintered material was evaluated for thermal and mechanical properties, and microstructures were examined using scanning electron microscopy (SEM), energy dispersive spectroscopy (EDS), transmission electron microscopy (TEM) and X-ray photo spectrometry (XPS). Similar work was done with NARloy-Z-D composites in parallel.

BLENDING OF NARLOY-Z WITH MWCNT BY BALL MILLING

Ball milling was expected to provide a means for physically incorporating MWCNTs into NARloy-Z powder. During the milling process, steel balls driven by a stirrer undergo high energy impacts. Powder particles trapped between the balls undergo high strain rate deformations. Initially, the metal powders undergo welding and grow in size. However, as the amount of deformation increases with longer milling times, the powders undergo more fracture than welding as cold work is accumulated in the particles, and the powders become finer (Ref. 5, 6). It was expected that the welding process would allow the MWCNTs to be incorporated into the NARloy-Z powder as was observed by Kim et al (Ref. 7).

NARloy-Z powder was blended with MWCNTs (from Pyrograf, Inc.) in the attritor shown in Figure 2. The vessel was nominally 10 cm dia. x 16.5 cm. A charge consisting of NARloy-Z and MWCNT powders of the appropriate ratio for the desired volume fraction of MWCNT was milled at a speed approximately 75% of the critical speed of the ball mill. Sufficient stainless steel balls were added to fill about two-thirds of the volume of the vessel. Liquid nitrogen, which also supplied the high purity nitrogen cover gas, was used to cool the vessel and to help prevent oxidation by keeping the temperature low. Blending was monitored for powder morphology and dispersion of MWCNT in the powder. Powder morphology and blending was examined in the SEM.

BLENDING OF NARLOY-Z WITH DIAMOND PARTICLES

The diamond powder was supplied by Diamond Innovations of Columbus, Ohio. The particle size was 40-60 μm and the thermal conductivity was expected to be 600-1000 W/m-K. NARloy-Z and diamond powders were blended in a Resodyne acoustic mixer at Applied Research Laboratory (ARL) at Pennsylvania State University.

Table 2: NARloy-Z-MWCNT and NARloy-Z-Diamond composites studied

Material/Process	**Vol.% (CNT/D)**	**Wt.% (CNT/D)**	**Density (gm/cc)**	**Characterization**
NARloy-Z baseline (FAST)*	0	0	9.13	Thermal conductivity, mechanical, microstructure
NARloy-Z-MWCNT (FAST)*	1	0.25	9.06	Thermal conductivity
	2	0.5	8.99	Thermal diffusivity
	5	1.25	8.78	Thermal conductivity, mechanical, microstructure
	10	2.5	8.44	Thermal conductivity, mechanical, microstructure
	20	5	7.75	Thermal diffusivity, microstructure
	40	10	6.38	Microstructure
NARloy-Z-MWCNT (Extrusion)	1	0.25		Microstructure, electrical resistivity
	5	1.25		Microstructure, electrical resistivity
	10	2.5		Microstructure, electrical resistivity
NARloy-Z-Diamond (FAST)*	10	2.5	8.44	Thermal conductivity, microstructure
	20	5	7.75	Thermal conductivity, microstructure
	40	10	6.38	Thermal conductivity, microstructure
*Parameters used for FAST: Temperature: 975^0 C, Pressure: 65 MPa, Heating rate: 10^0 C, Holding time at temperature: 20 minutes, Furnace cooled				

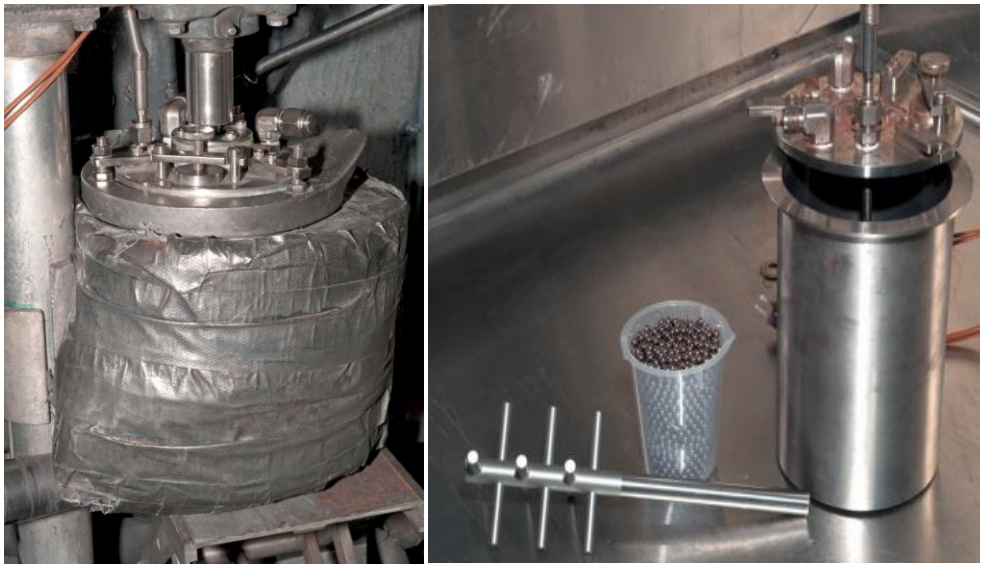

A. Attritor ready for operation B. Attritor parts

Figure 2: Attritor used for blending of NARloy-Z and MWCNTs (GRC)

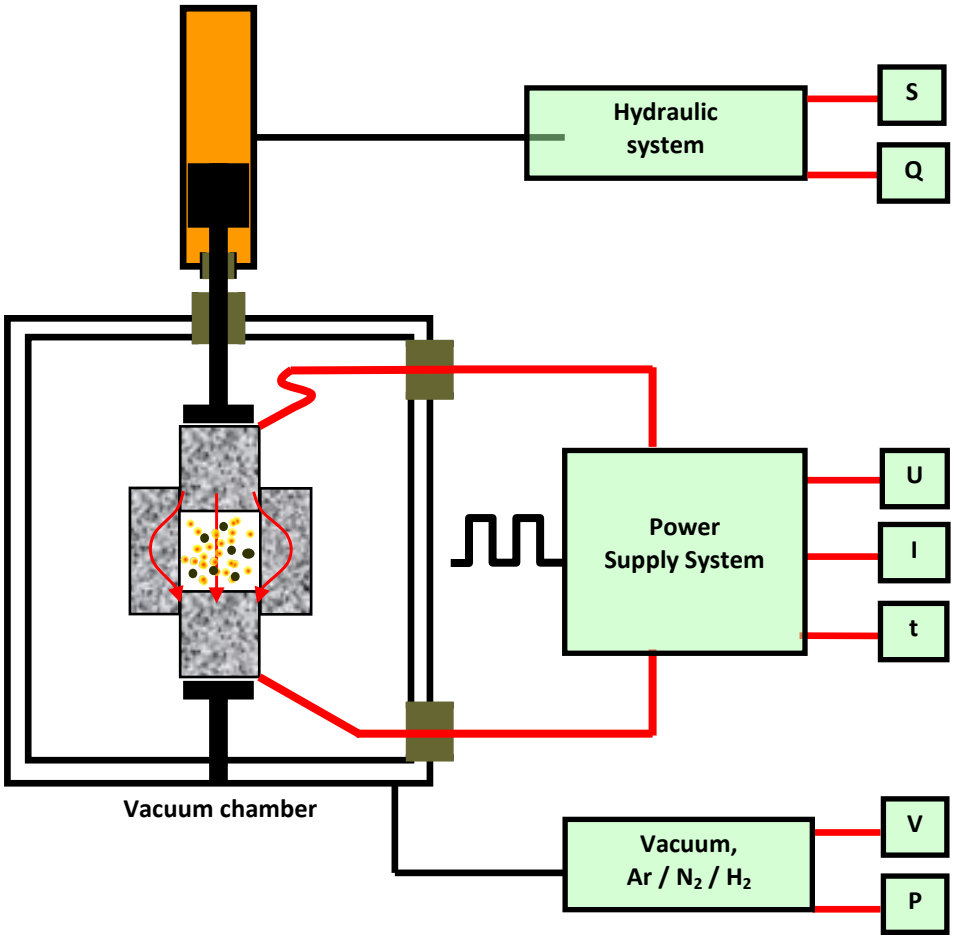

3A. FAST schematic

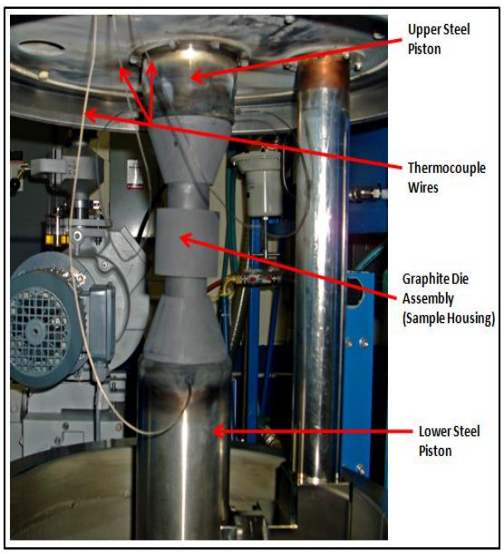

3B. FAST apparatus at ARL-Penn State 3C. Sintering at high temperature using FAST

Figure 3: Field Assisted Sintering Technology (FAST)

SINTERING

Blended NARloy-Z-MWCNT powders with varying amounts of MWCNTs were processed at ARL - Penn State. The powders were sintered at 975 °C using FAST, which is shown schematically in Figure 3. The process consisted of placing a NARloy-Z-MWCNT powder blend in the graphite die. Pressure was applied via an upper and lower punch. The pulsed DC current flows through the punches and the die. The current through the die provides radiant heating to the powder while current flowing through the powder produces resistive Joule heating. The combined effect of pressure, temperature and localized heating at the contact points in the powder resulted in a high sintering rate. Disks 80 mm diameter x 6 mm thick were produced. Test specimens for evaluating mechanical and thermal properties and microstructure were machined from these disks. NARloy-Z-D powder blends were also sintered using the same FAST parameters as NARloy-Z-MWCNT.

The NARloy-Z-MWCNT composite disks were heat treated as specified for maximum NARloy-Z strength. The heat treatment consisted of solution treatment at 900°C (1650°F) for 2 hours with a gas quench followed by an aging treatment at 482°C (900°F) for 4 hours with furnace cooling. The heat treatments were done in either vacuum or an argon atmosphere. Heat treated samples were machined into test specimens for determining tensile properties at GRC, thermal properties at Thermophysical Properties Research Laboratories (TPRL, West Lafayette, Indiana). Additional thermal diffusivity measurements and microstructure analyses were conducted at NASA-MSFC.

EXTRUSION OF NARLOY-Z-MWCNT

The extrusion process tends to align the MWCNTs in the direction of extrusion. Aligned composites are expected to show higher thermal and electrical conductivities than randomly oriented composites obtained by straight sintering. Extrusion also imparts a large amount of work to the material. It was hoped that this work would help to break up the MWCNT clumps. The purpose of this task was to verify if this was the case with NARloy-Z-MWCNT composites.

NARloy-Z powder was blended with 1, 5, and 10 volume percent MWCNT and encapsulated in copper extrusion cans under vacuum. The cans were extruded at 500-600 °C to reduce the cross section. The extrusions were re-canned and extruded a second time. The target minimum reduction in area was 95%. Cross-sectional samples were mounted and polished to reveal the distribution of the MWCNTs in the extrusions.

THERMAL PROPERTY MEASUREMENT

Thermal diffusivities (α) as a function of temperature were measured using laser flash techniques by two laboratories. The testing at TPRL was closely duplicated at NASA-MSFC. Bulk density (ρ) values were calculated at room temperature from each sample's geometry and mass. Specific heat (C_P) as a function of temperature was measured using a differential scanning calorimeter. The thermal conductivity (λ) value at temperature T was calculated using the equation

$$\lambda (T) = \alpha(T)\, C_P(T)\rho \qquad \text{Eq. 1}$$

The thermal conductivity of the NARloy-Z-D composites was measured on a Netzsch Nanoflash - laser flash method by Momentive Performance Materials.

MEASUREMENT OF MWCNT THERMAL CONDUCTIVITIES

The thermal conductivity of MWCNTs supplied by Pyrograf, Inc. used in this study and several other suppliers were measured at Vanderbilt University. The method has been used for individual single wall carbon nanotubes (SWCNT) and various nanowires and nanoribbons (Ref. 8-11) with good success.

An individual MWCNT sample was placed between two suspended membranes serving as a heat source and a heat sink (Fig. 4). The power dissipation and the temperature rise of the heat source and sink were measured, from which the thermal conductivity of the sample was calculated after the

dimension of the sample was determined using electron microscopy. Individual thermal conductivity measurements were an effective value that included additional resistances from the contact between the sample and membranes. For select samples, the contacts' thermal resistances were calculated and eliminated through multiple measurements of the same sample with different lengths between the heat source and heat sink (Ref. 12). For most samples, only a single measurement was made to screen the various MWCNTs quickly, and the contact resistance was estimated based upon the values obtained for the complete thermal conductivity tests.

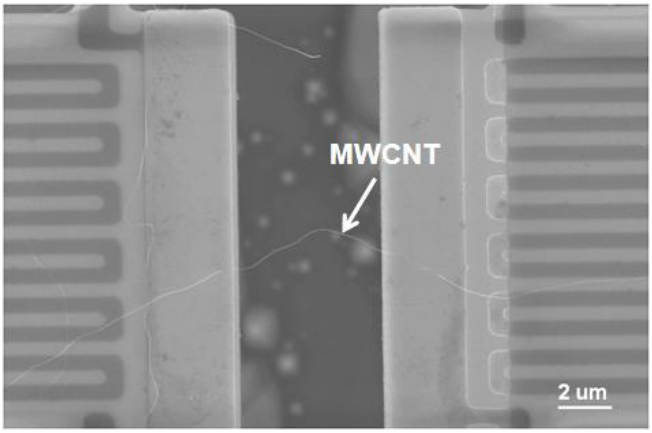

Figure 4: A MWCNT sample on the measurement device. Two suspended membranes with integrated platinum coil serving as heat source/sink. The platinum coils serves as both an electric heater and a resistance thermometer.

ADDITIONAL CHARACTERIZATION OF MWCNTS

Following discovery of the low thermal conductivity of the MWCNT samples, additional characterization was performed to understand the low results. A Raman spectroscopy study was performed on samples from all suppliers to establish the general quality of the MWCNTs. Raman Spectroscopy provides information of the relative abundance of the sp^2 bonds (G peak, signature of graphitic layers) and the sp^3 bonds (D peak, signature of defects). Prior observations have indicated that a low disordered to graphite (D/G) peak height ratio is indicative of a good MWCNT with high thermal conductivity. For good quality tubes, the D/G ratio should be very small. This is because the D peak can only be created by defects in the carbon layers that make up the tube wall (Ref. 12, 13).

SEPARATION AND COATING OF MWCNTS

MWCNTs tend to agglomerate naturally and form clumps that do not break up very well during blending. Hence it is important to separate the MWCNTs and keep them separated before blending to take full advantage of their properties. A number of techniques have been used to separate the MWCNTs by functionalizing them with both organic and inorganic species (Ref.14-19). The surface oxidation and metallization of MWCNTs permits fabrication of surface modified MWCNTs which can provide good a bond between the matrix and MWCNT. Acid oxidation of MWCNTs is preferred since it proceeds homogeneously and favors the formation of carboxylic acid moieties over weakly acidic groups such as hydroxyl moieties (Ref. 20). These surface carboxylic groups not only help make the MWCNTs well-dispersed in the matrix, but also provide a site for the nucleation of metal on the MWCNTs after separation. Therefore, acid oxidation is the starting point for the vast majority of reports pertaining to the wet chemical modification of MWCNTs such as electroless plating (Ref. 19, 21) and was used in this study.

Before electroless plating, pretreatments including oxidation, hydrophilic treatment, sensitizing treatment, and activating treatment were performed on the MWCNTs. The dispersion and wetting characteristics were improved by introducing –COOH groups on the surface. Acid oxidation of MWCNTs

was carried out by immersing the MWCNTs in a 3:1 mixture of concentrated sulfuric acid (H_2SO_4) and concentrated nitric acid (HNO_3) at 80 °C for 10 h. The MWCNTs were washed with distilled water and separated from the liquid by centrifugation. The surface of a MWCNT has low chemical reactivity and does not act as a catalyst or nucleation site for the deposition of metal coating unless it is activated. Therefore, a pre-activation (surface catalyst) step was needed. This was accomplished by immersing the MWCNTs for 30 min. in an aqueous solution of 0.1M $SnCl_2$–0.1M HCl, followed by rinsing in distilled water. The MWCNTs were then immersed for a further 30 min. in an aqueous solution of 0.0014M $PdCl_2$-0.25M HCl (Ref. 21). The activated MWCNTs were washed with distilled water and separated from the solution by centrifugation. Finally, the activated MWCNTs were introduced into the electroless bath and coated with Cr.

RESULTS

The results obtained in this investigation are presented below. The primary focus was thermal conductivity measurements and microstructure-property relationships. Tensile properties were tested and reported for selected NARloy-Z-MWCNT composites to observe the general response of the composites.

BALL MILLING

Prior ball milling of pure Cu – MWCNT composites had shown that the welding phase of the ball milling persisted for an extended period of time. The alloyed NARloy-Z powders, however, work hardened much faster, and the welding phase appeared to end by 60 minutes (Figure 5). As a result, the time for

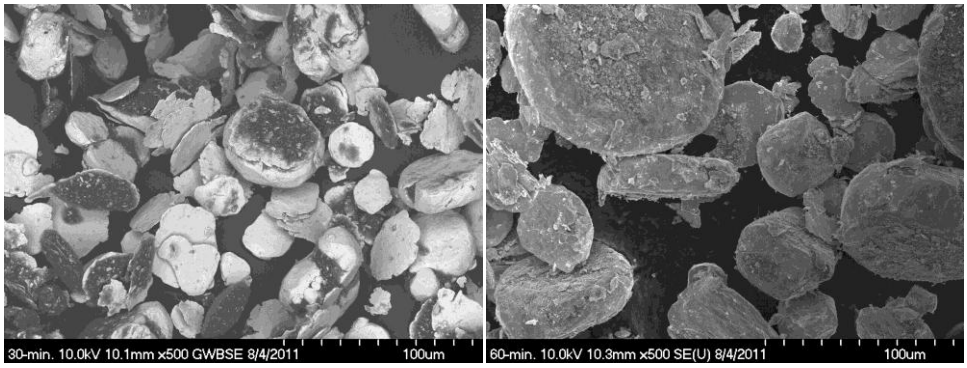

(a) 30 minutes (b) 60 minutes

Figure 5: Powder morphology evolution during ball milling for NARloy-Z-10%MWCNT

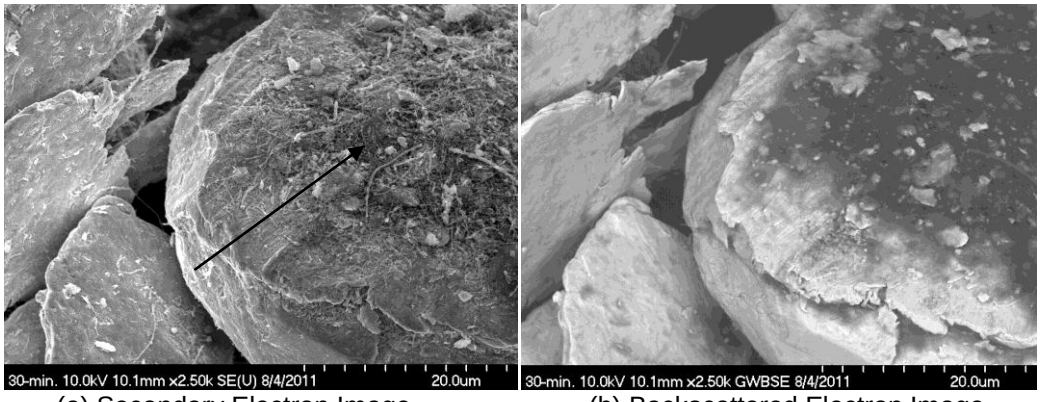

(a) Secondary Electron Image (b) Backscattered Electron Image

Figure 6: Typical NARloy-Z – MWCNT Composite Powder Particle Surfaces

milling was decreased to 45 minutes to maximize the incorporation of MWCNT into the NARloy-Z while minimizing the fracture of the particles that could damage the MWCNTs. It was noted that the ball milling did not completely incorporate the MWCNT into the NARloy-Z. As Figure 6 shows, a portion of the MWCNTs were left on the surface of the powder particles as remnant clumps (shown by arrow). These clumps appear dark in backscattered electron images (Figure 6b).

TENSILE PROPERTIES

Tensile test results for NARloy-Z baseline and NARloy-Z-MWCNT composites are shown in Table 3. Stress-strain curves for base line and 5% MWCNT are shown in Figure 7. The NARloy-Z baseline sintered sample produced by FAST had lower yield strength and comparable ultimate tensile strength (UTS) to wrought NARloy-Z. NARloy-Z-5% MWCNT and 10% MWCNT failed shortly after yielding but had good yield strengths. Figure 8A shows fractured tensile specimens, and Figure 8B shows fractured surfaces. The composites demonstrated brittle fracture with little to no necking. The fracture surfaces were also very noticeably darker, indicating that MWCNTs were likely concentrated on the fracture surface.

Table 3: Tensile properties of NARloy-Z-CNT composites

% MWCNT	Average Yield (MPa)	Average UTS (MPa)	Average Elongation (%)	Average R.A. (%)
0	88.2	271.7	31.3	61.2
5	105.9	124.7	1.6	1.2
10	97.8	107.5	0.8	0.8

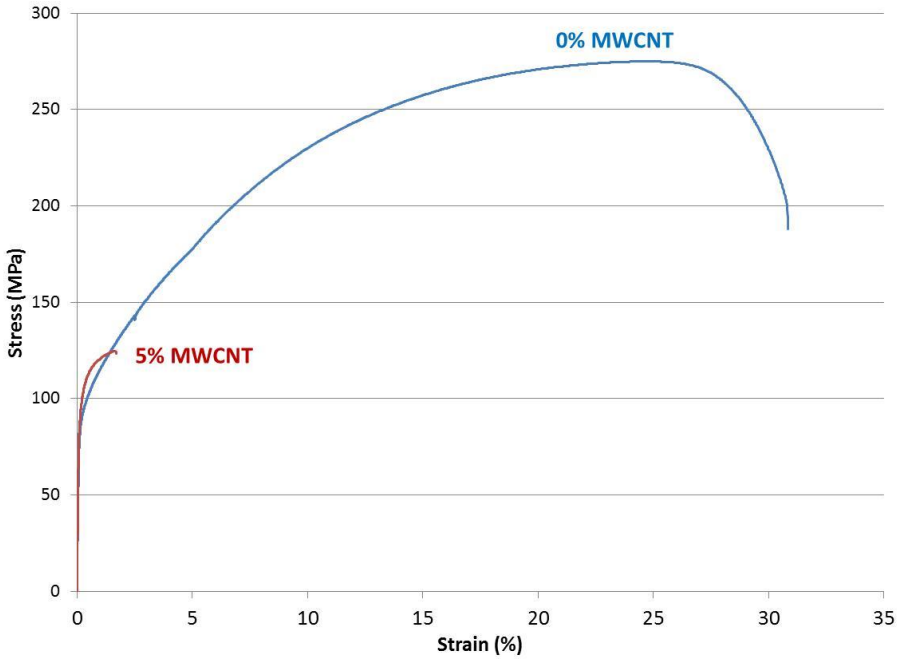

Figure 7: Stress-strain curves for baseline pure NARloy-Z (0% MWCNT) and NARloy-Z-5% MWCNT

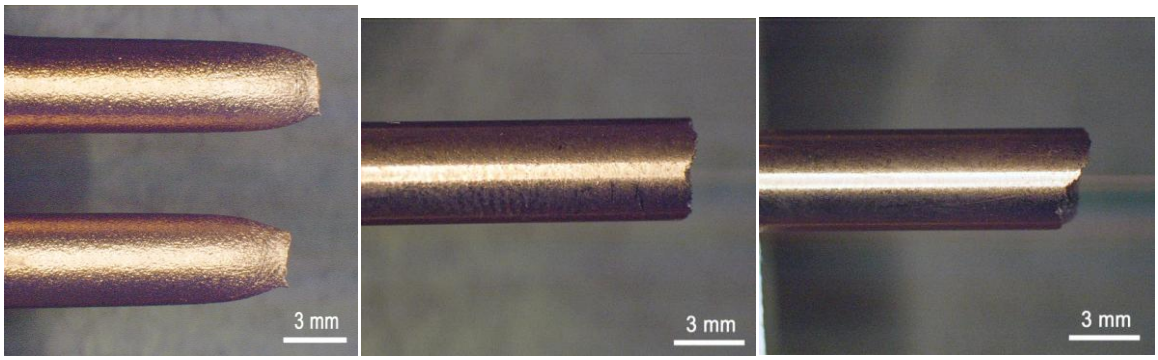

0% MWCNT 5%MW CNT 10% MWCNT

Figure 8A: NARloy-Z-CNT tensile specimens

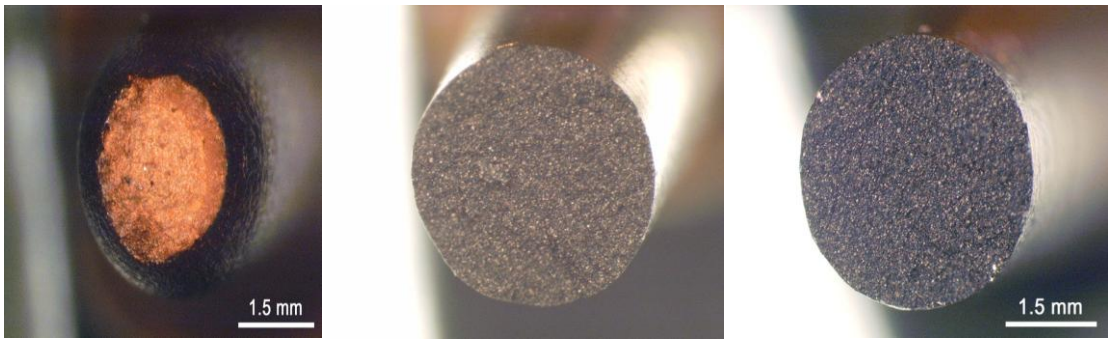

0%MWCNT 5% MWCNT 10% MWCNT

Figure 8B: NARloy-Z-MWCNT tensile fracture surfaces

THERMAL PROPERTIES

The thermal conductivities measured at TPRL are shown in Figure 9 for the NARloy-Z baseline, NARloy-Z-5% CNT and NARloy-Z-10% CNT samples. Figure 10 shows thermal diffusivity data from TPRL, and Figure 11 shows thermal diffusivity data from NASA-MSFC. The laser flash method was used in both cases. The data were quite similar, and the general trend in both data sets was the same. Thermal diffusivity and thermal conductivity decreased as the volume fraction of MWCNTs increased.

Since the densities of MWCNTs and diamond are much lower than NARloy-Z, adding MWCNT or diamond decreases the density of the composites. The thermal conductivity of each NARloy-Z-D composite was divided by the measured density to provide specific properties. The results are shown in Figure 12. The increase in thermal conductivity appeared to be proportional to the diamond content and was 69% higher at 40 vol.% diamond. The increase in specific thermal conductivity was much higher (142%), since the composite density decreased significantly with increasing diamond content.

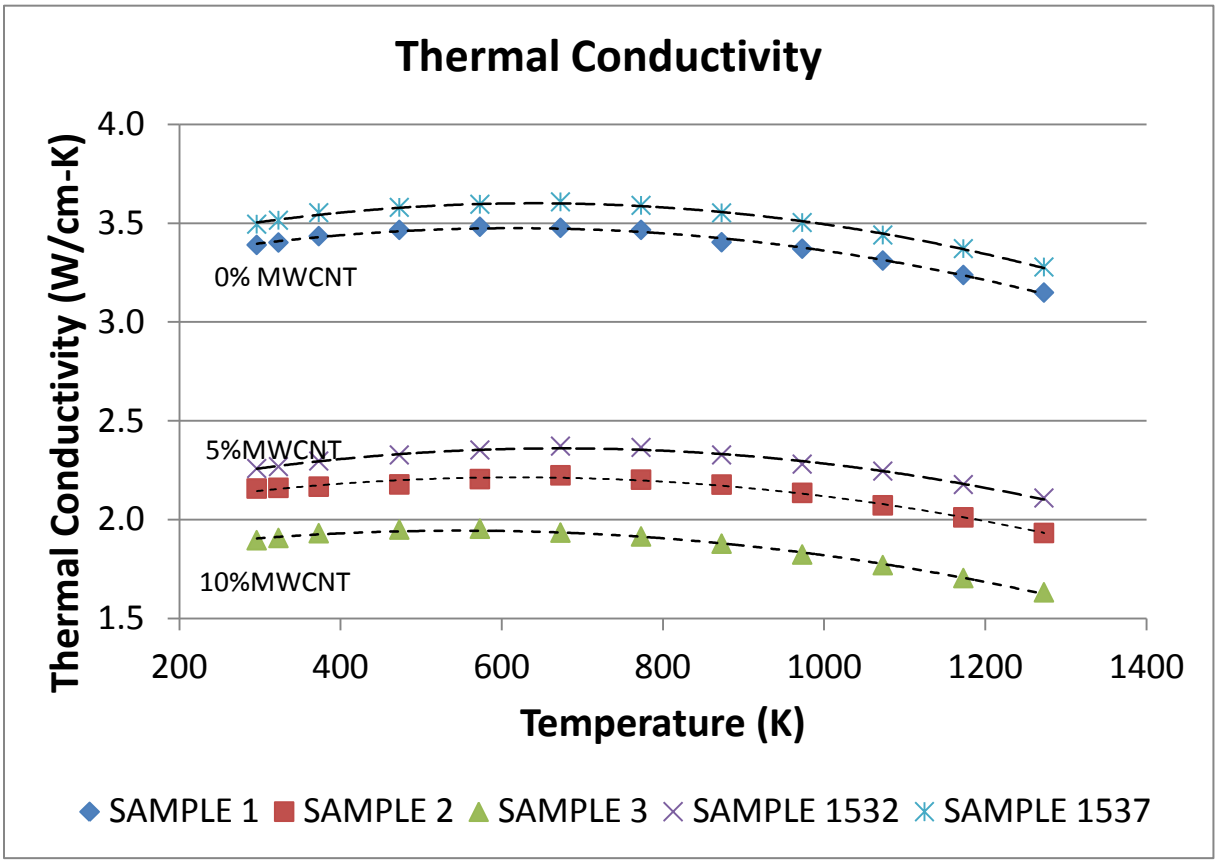

Figure 9: Thermal conductivity of NARloy-Z-CNT composites (TPRL)

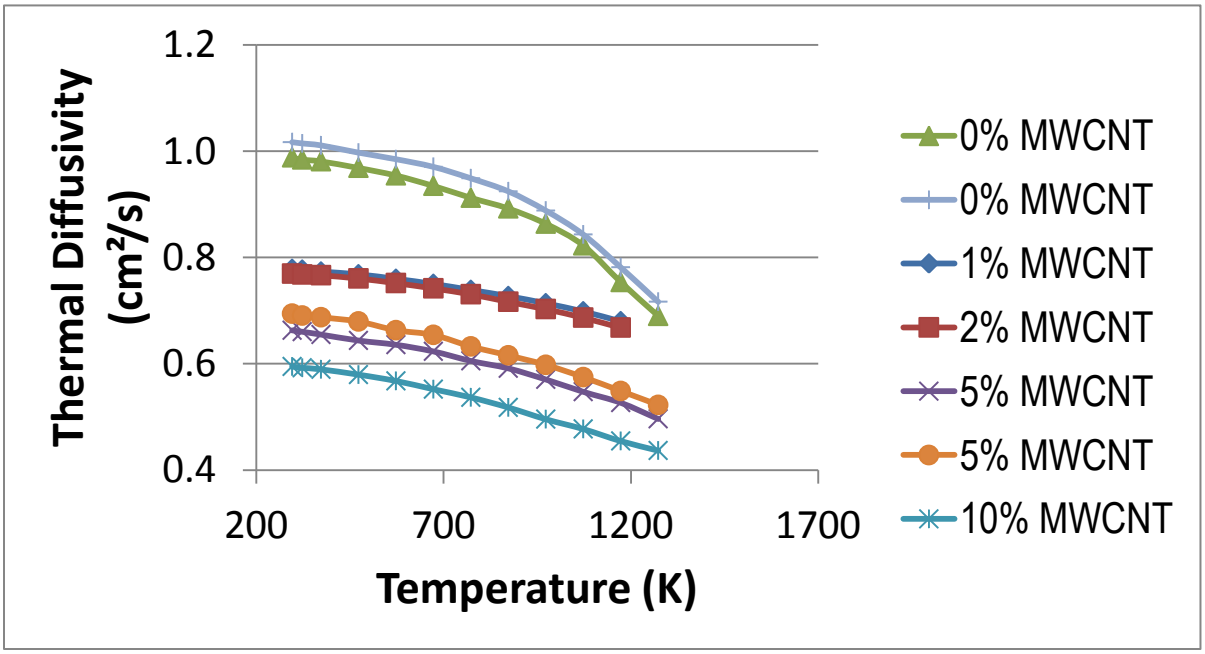

Figure 10: Thermal diffusivity data generated at TPRL (Ref. 9)

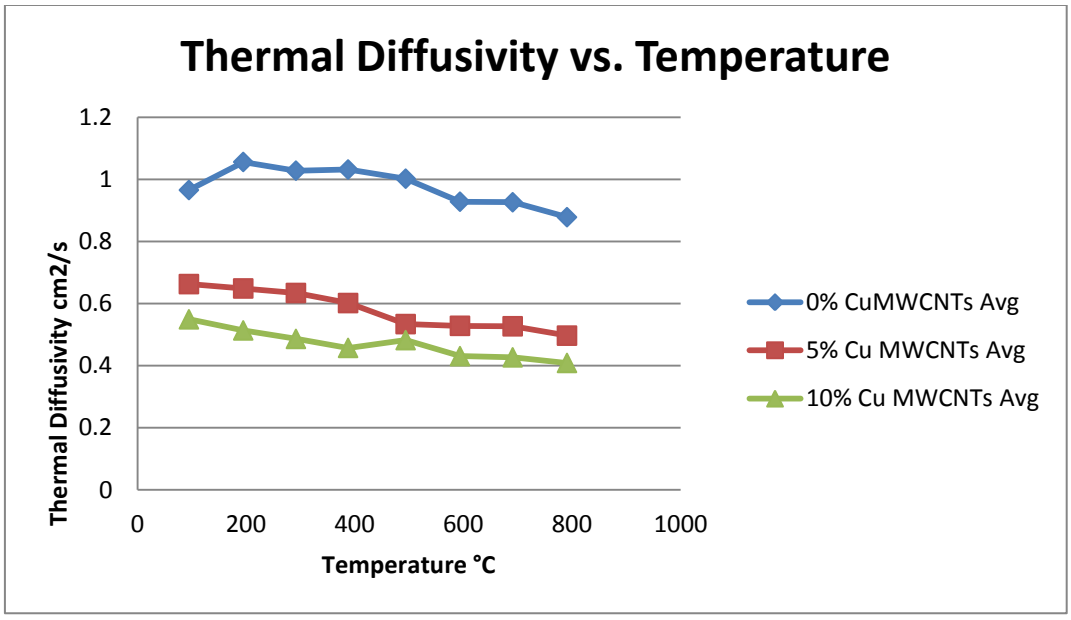

Figure 11: Thermal diffusivity data generated at NASA-MSFC (Ref. 10)

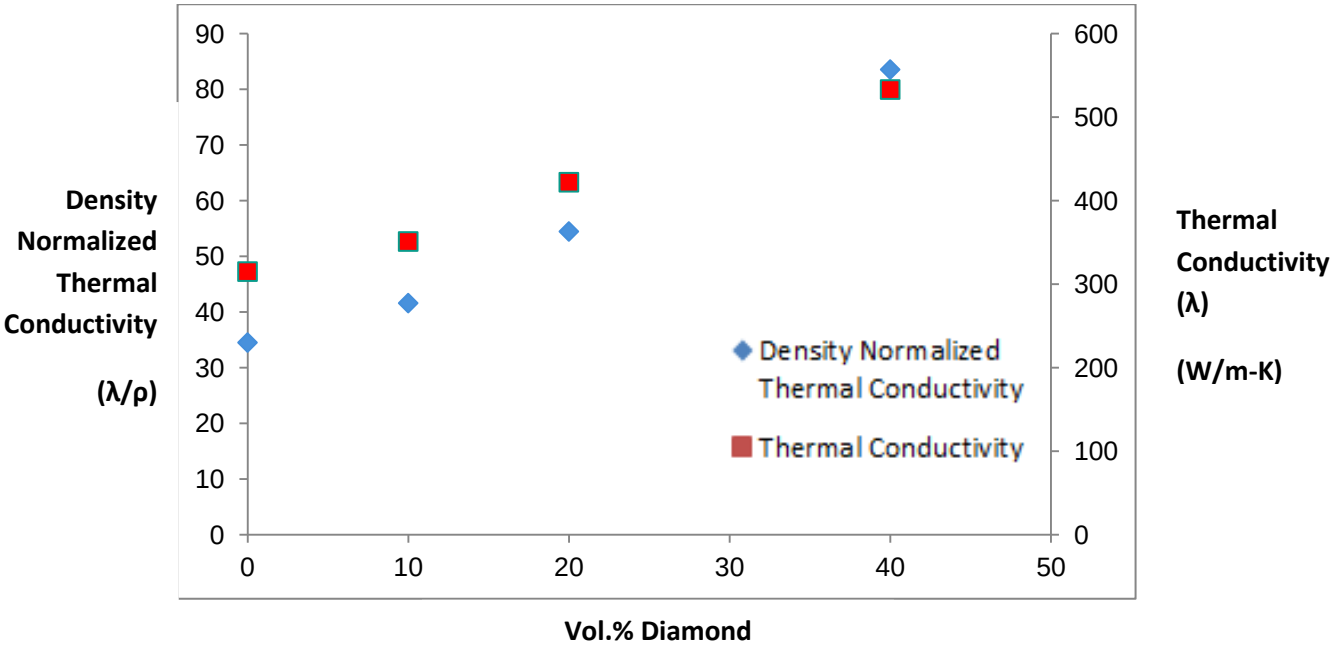

Sample	Vol. % Dia	Thermal Conductivity (λ), W/mK	Density, ρ (gm/cc)	λ/ρ
CuAgZr (NARloy-Z)	0	315	9.13	34.50164
CuAgZr+10 vol % D	10	351	8.44	41.58768
CuAgZr + 20 vol % D	20	422	7.75	54.45161
CuAgZr + 40 vol % D	40	533	6.38	83.54232

Figure 12: Thermal conductivity of NARloy-Z-D composites at room temperature. Both normal (λ) and density normalized (λ/ρ) are shown.

MICROSTRUCTURE ANALYSIS

Figure 13 shows SEM images of NARloy-Z-MWCNT microstructures. It was evident that MWCNTs remained segregated on the surfaces of the powder rather than being incorporated into the powder particles. As a result, they appear at the prior particle boundaries (PPBs).

SEM images and zirconium X-ray maps are shown Figures 14 and 15 for the baseline NARloy-Z and NARloy-Z-2% MWCNT samples, respectively. Figure 16 shows a similar micrograph for NARloy-Z-20% diamond composite. Migration by diffusion during processing of Zr to MWCNT and diamond particles was evident. Such migration was not observed in the pure NARloy-Z base line material where Zr is fairly evenly distributed as Cu-Zr precipitates (Figure 14).

XPS ANALYSIS

An XPS analysis was conducted in a microprobe to identify compounds at the interfaces such as ZrC that would lower the contact thermal resistance at the MWCNT-matrix interface as predicted by the quantum mechanics-based model. Results are shown in Figures17 and 18. The de-convoluted Zr 3d spectrum showed three different forms of Zr: zirconium oxide (ZrO_2), zirconium carbide (ZrC), and metallic zirconium (Zr), which is dissolved in the matrix. The C 1s spectrum showed a peak for the carbon-carbon bonds expected for MWCNTs. A small peak at a lower binding energy was observed and signified the presence of ZrC.

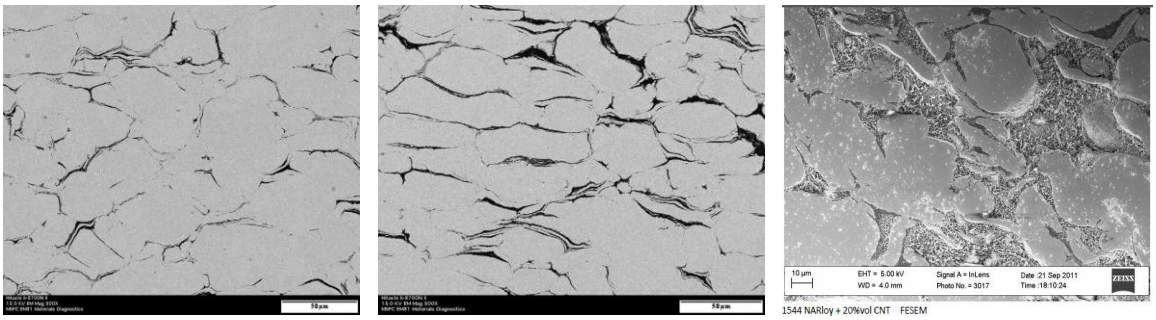

NARloy-Z-5%CNT NARloy-Z-10%CNT NARloy-Z-20%CNT

Figure 13: SEM images of NARloy-Z-CNT composites

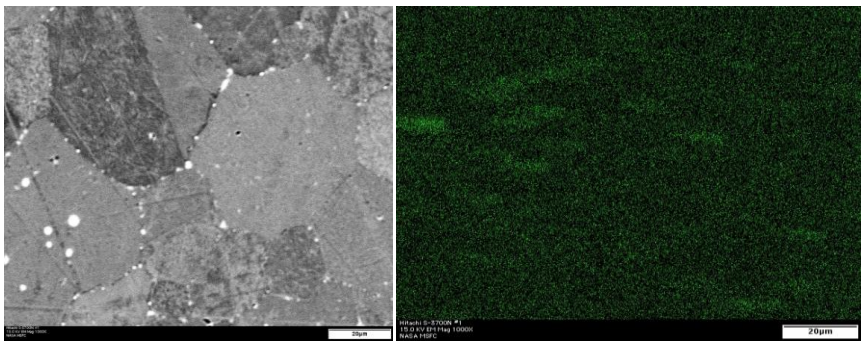

Figure 14: SEM-EDS analysis of NARloy-Z base line material showing zirconium (Zr) elemental map. Note the relatively uniform distribution of Zr.

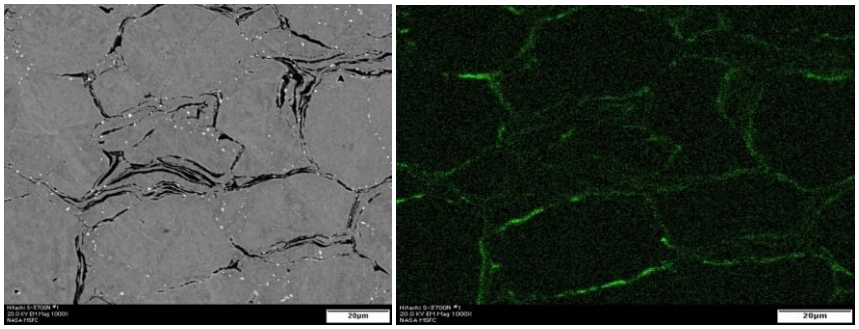

Figure 15: SEM-EDS analysis of NARloy-Z-2% CNT showing Zr elemental map. Note the segregation of MWCNTs at prior particle boundaries and migration of Zr to the same area.

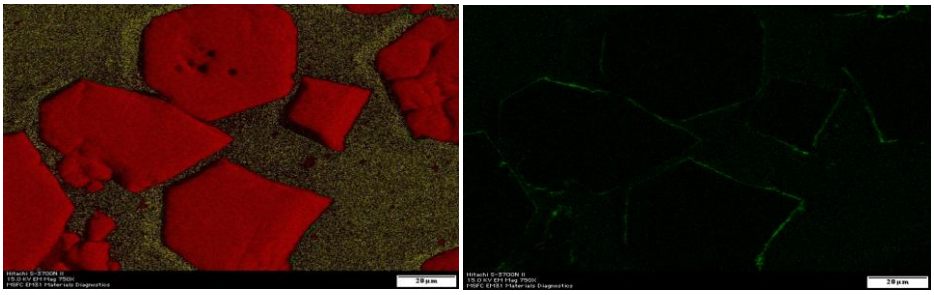

Figure 16: SEM-EDS analysis of NARloy-Z-20% diamond showing Zr elemental map. Note the migration of Zr to diamond-NARloy-Z matrix interface.

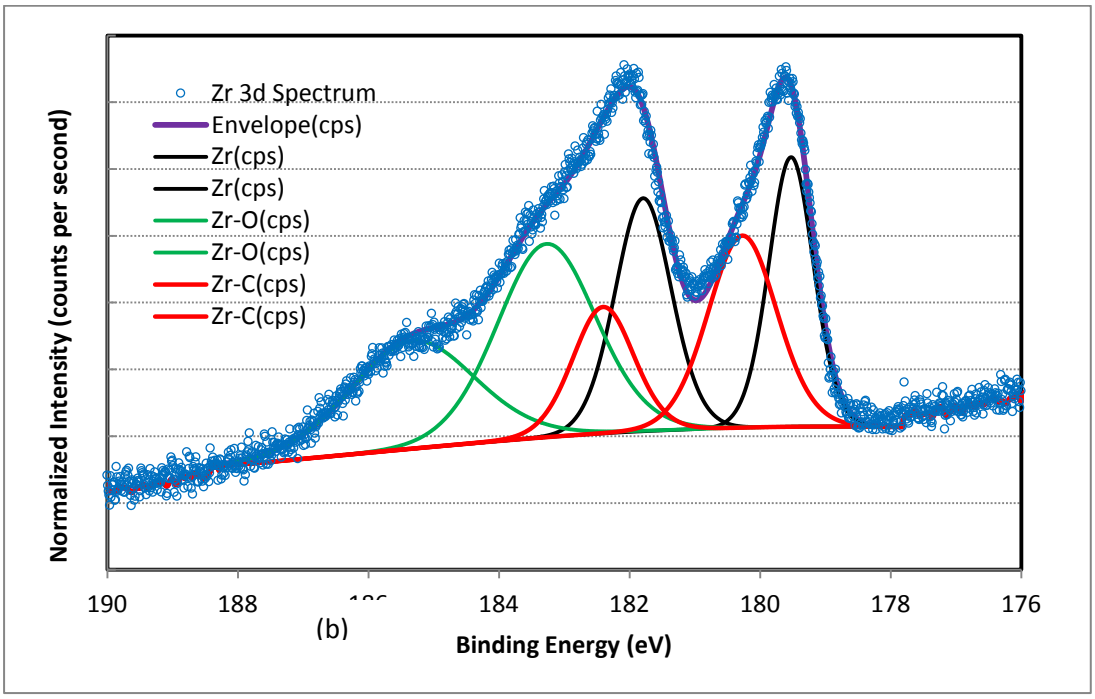

Figure 17: De-convolution of the Zr 3d XPS Spectrum for NARloy-Z-1%MWCNT interface.

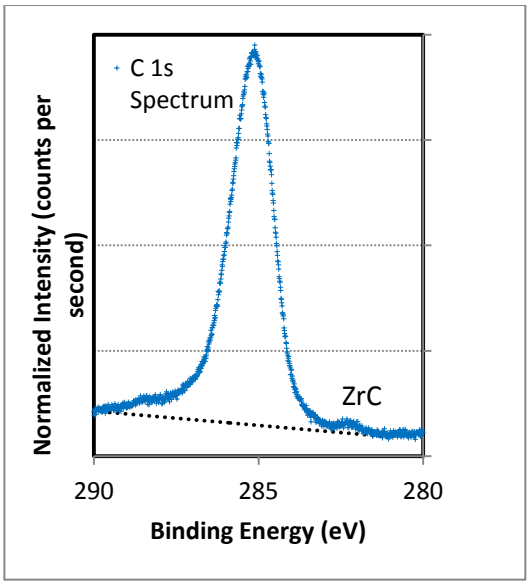

Figure 18: XPS C 1s spectrum showing a small ZrC peak for a 1% MWCNT-NARloy-Z interface. This is the same interface as the results presented in Figure 17.

A similar analysis was conducted with NARloy-Z-D composite material, and results are shown in Figure 19 along with the results for NARloy-Z-MWCNT for comparison. It appears that zirconium migrated towards carbon in both cases and formed ZrC as desired. The peaks are rather weak, which indicates that these are likely nanolayers of ZrC, insufficient to produce strong peaks.

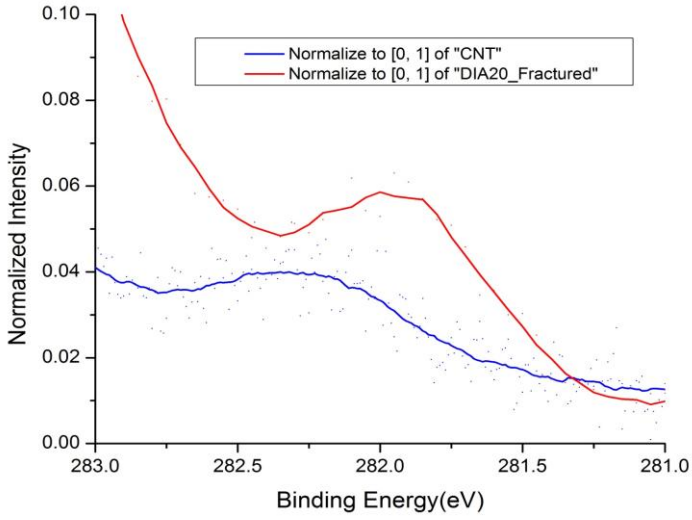

Figure 19: XPS Analysis of NARloy-Z-1%MWCNT and NARloy-Z-20%Diamond composites showing ZrC peaks. Peak height for NARloy-Z-MWCNT is smaller because of a thinner ZrC layer. Note: NARloy-Z-Diamond specimen was hard to polish and was fractured to expose interface.

EXTRUDED NARLOY-Z-MWCNT COMPOSITES

A representative NARloy-Z-MWCNT transverse extruded microstructure is shown in Figure 20. The total reduction in area of the extrusions was 96%. As can be seen in Figure 20, there were dark areas identified as MWCNT clumps and cracks as well as lighter areas identified as NARloy-Z. Apparently, even with the combination of ball milling and severe reduction in area, the MWCNTs were largely unincorporated into the NARloy-Z matrix. The microstructures were similar to the FAST-consolidated composites.

The electrical resistivities for both NARloy-Z-MWCNT and previously tested Cu-MWCNT extrusions are presented in Figure 21. Electrical resistivity of NARloy-Z appears to increase with MWCNT additions much faster than pure copper, probably due to poor bonding between particles and a generally less blended microstructure. Thermal conductivity measurements were not pursued since it was considered unlikely to be good based upon the highly segregated and cracked microstructure.

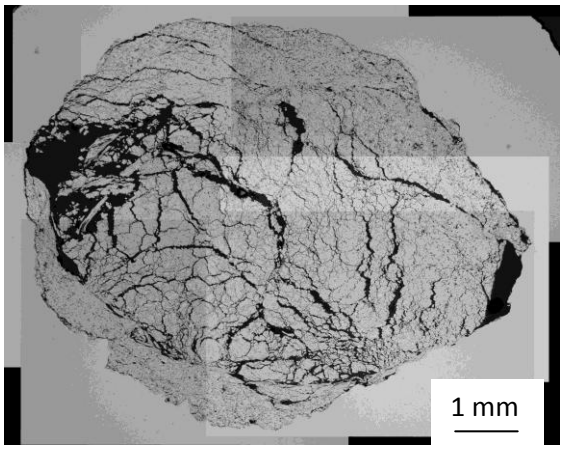

Figure 20: Macrograph of extruded NARloy-Z-10%CNT composite

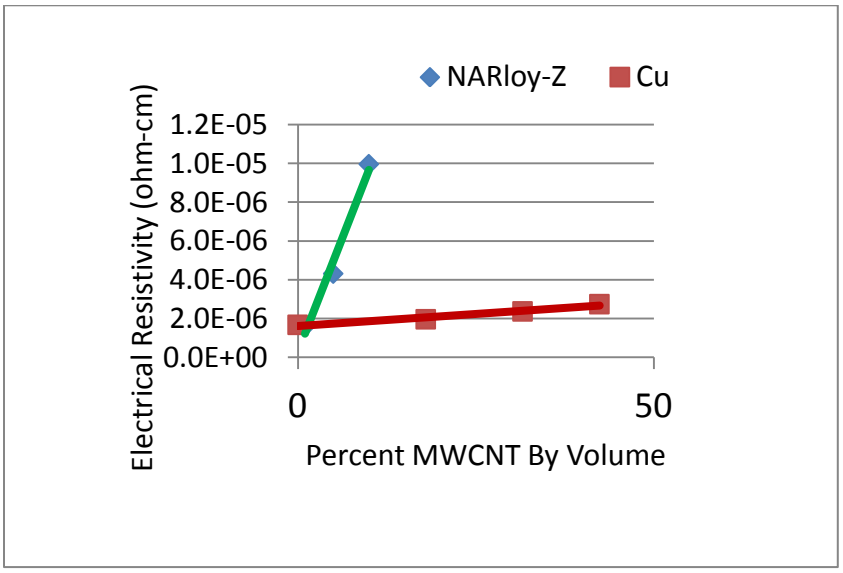

Figure 21: Electrical resistivity of extruded NARloy-Z-CNT and Cu-CNT composites

MWCNT THERMAL CONDUCTIVITY AND QUALITY

Initially only Pyrograf MWCNTs were tested. The results were surprisingly low with a room temperature thermal conductivity around 50 W/m-K as opposed to >300W/m-K for NARloy-Z and 400 W/m-K for pure Cu. Since it has been reported that the thermal conductivity of individual MWCNTs could be very high (>2000 W/m-K based upon Ref. 13), it was decided to obtain additional MWCNTs for testing and possible substitution for Pyrograf MWCNT in future composites.

The results are shown in Figure 22. The thermal conductivity values of most MWCNTs are very low relative to the highest reported value. The highest thermal conductivity was obtained by MWCNTs from Case Western Reserve University (CWRU), which was slightly over 200 W/m-K. The other thermal conductivities are effective thermal conductivities, which include the effects of the contact resistances. They are lower than the actual thermal conductivities. Using the contact resistances obtained for the CWRU samples, which had similar effective thermal conductivities, the intrinsic thermal conductivity of the MWCNTs were still below 100 W/m-K. They definitely were not comparable to Cu and did not approach the values reported in the literature.

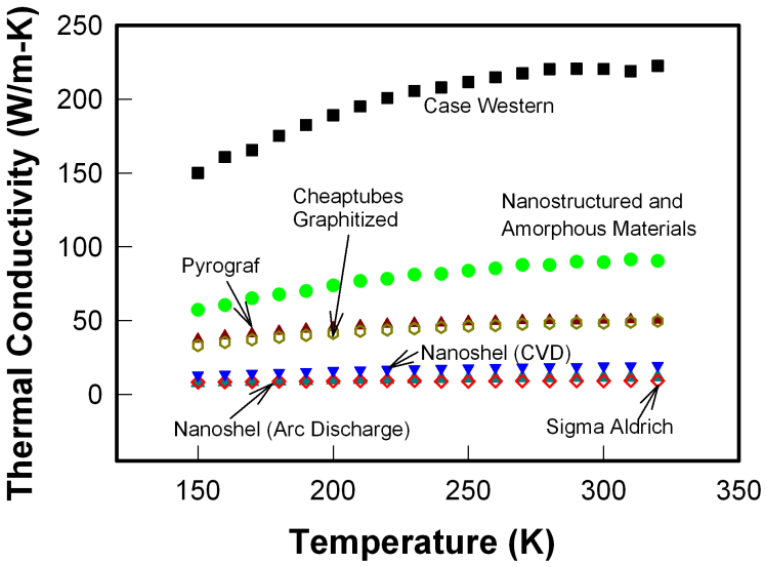

Figure 22: Measured thermal conductivity of different MWCNT samples. For samples from some suppliers, multiple measurements have been performed and the values are similar. The result for the Case Western sample is intrinsic thermal conductivity while the others are effective thermal conductivities

A Raman spectroscopy study was performed on samples from all suppliers to establish the general quality of the MWCNTs. Raman shifts for MWCNTs obtained from two suppliers (Nanoshel and Cheap Tubes) are shown in Figure 23. D/G results for all vendors are shown in Table 4. Generally, a D/G peak ratio of 0.02 indicates a low defect concentration in the MWCNTs (Ref. 22). It can be seen that, for all samples, the D/G ratios were four to fifty-five times larger, which is inferred to mean that the MWCNTs were of generally poor quality. The thermal conductivities of MWCNTs from suppliers with very high D/G ratios were not measured in most cases due to the expected large amount of defects, which lower thermal conductivity.

TEM images are shown in Figure 24. They indicate significant structural imperfections that limited the phonon mean free path, and hence reduced the thermal conductivity.

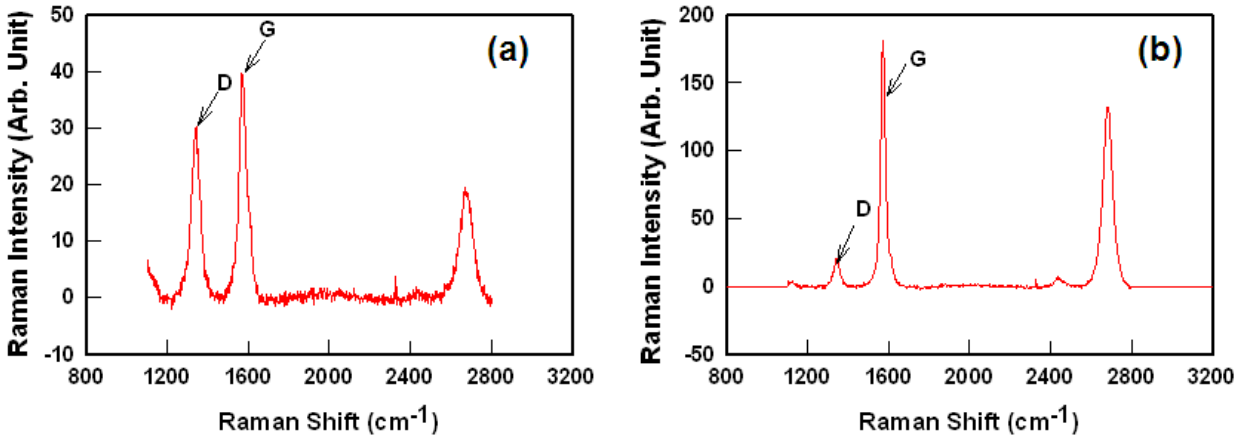

Figure 23: Raman spectroscopy results for (a) Nanoshel CVD MWCNTs with a large D/G ratio and (b) Cheap Tubes graphitized MWCNTs with a low D/G ratio.

Table 4: Raman Spectroscopy results for different vendors of MWCNT

Sample #	Vendors	D/G ratio
1	Cheap Tubes	0.59
2	Cheap Tubes (Graphitized, 80 nm nominal diameter)	0.13
3	Cheap Tubes (Graphitized, 30 nm nominal diameter)	0.21
4	Helix Material Solutions	0.62
5	Io-li-tec	0.59
6	mk Nano	0.59
7	NanoCs	0.77
8	Sigma Aldrich	0.09
9	Ted Pella	0.86
10	SES Research	0.50
11	Nanostructured and Amorphous Materials	0.54
12	US Research Materials Inc.	0.58
13	Nanoshel (CVD MWCNTs)	0.82
14	Nanoshel (Arc Discharge MWCNTs)	0.18
15	General Nano	1.10
16	**Pyrograf**	**0.26**
17	Case Western Reserve University	0.47

From these studies, we can conclude that even though high thermal conductivities were expected and have been reported for MWCNTs, most available MWCNTs have bonding and structural defects, which have lead to much lower thermal conductivities than expected. To have a successful NARloy-Z-MWCNT composite with enhanced thermal conductivity, a MWCNT source which can deliver very high quality MWCNTs with thermal conductivity > 1000 W/m-K consistently needs to be first identified.

SEPARATION AND COATING OF MWCNT

XPS studies confirmed that nitric acid could create various oxygen containing functional groups such as -COOH, -OH, and C=O on the surface of the carbon nanotubes (Figure 25). These functional groups can greatly modify the wettability and further increase the absorption velocity of Sn^{2+} from the sensitizing solution to the surface. H_2SO_4 can absorb the water produced by HNO_3 and carbon nanotubes and makes the reaction continuous (Ref. 20). During the sensitization process, Sn^{2+} ions were deposited on the surface of the MWCNTs. When introduced in the activation solution, Pd^{2+} ions were reduced to Pd by

Sn^{2+}. These Pd particles were uniformly distributed on the surface of the nanotubes and acted as catalytic centers for chromium metal nucleation and deposition.

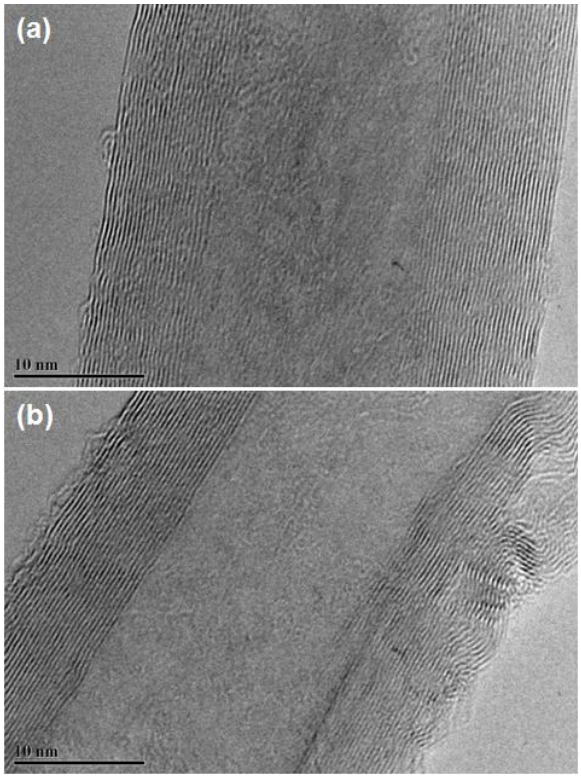

Figure 24: TEM micrograph of a MWCNT at different positions. While the tube structure in (a) is good, there are significant structural defects in (b), which reduce the thermal conductivity.

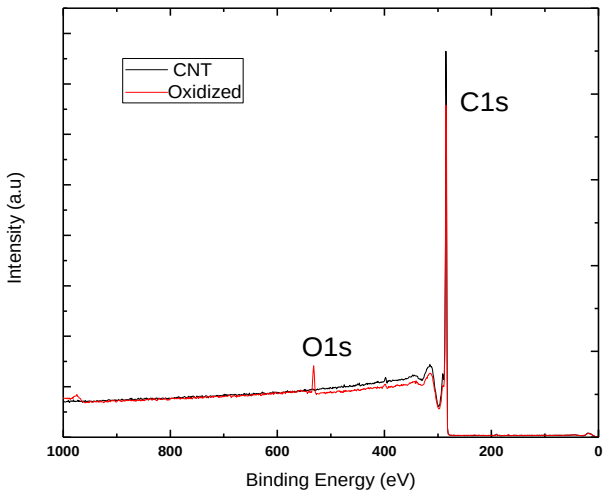

Figure 25: XPS survey scan for as-received MWCNTs and acid oxidized MWCNTs

An electroless plating bath comprised of chromium acetate salt with chromium fluoride and chromium chloride (Ref. 24) was used for Cr plating. The pH was varied to produce both basic and acidic conditions. Under basic conditions, formaldehyde was used as the metal ion reducing agent, and under acidic conditions, sodium hypophosphite was used for the same purpose. Different plating durations were used to vary the amount of Cr deposited.

Chromium coating resulted in a nanothick layer of metal on the surface of individual MWCNTs after oxidation and electroless plating, as is evident in Figures 26. Further chemical analyses were done by XPS using the Cr-2p peaks in the energy range of 574-576 eV. Peak fitting revealed the oxidation of the freshly deposited metal into mixed oxides and hydroxides. Only 10-15% of the deposited Cr remained metallic Cr after 1 h of electroless plating (Figure 27). The oxidation of chromium might be occurring during the plating from solution or during the washing stage after plating. It also might be oxidation that occurs upon exposure to air.

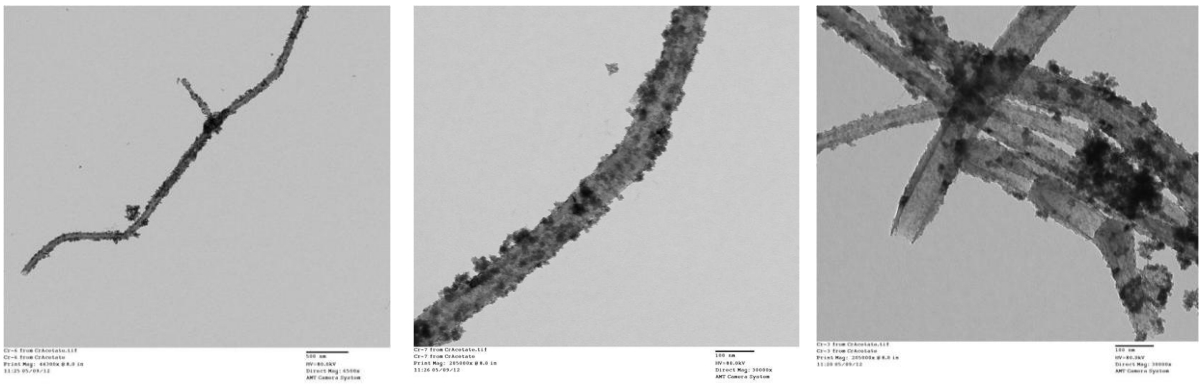

Figure 26: TEM images showing coating of metal from electroless plating method. ~20 nm thick layer of metallization can be observed in individual CNT surface.

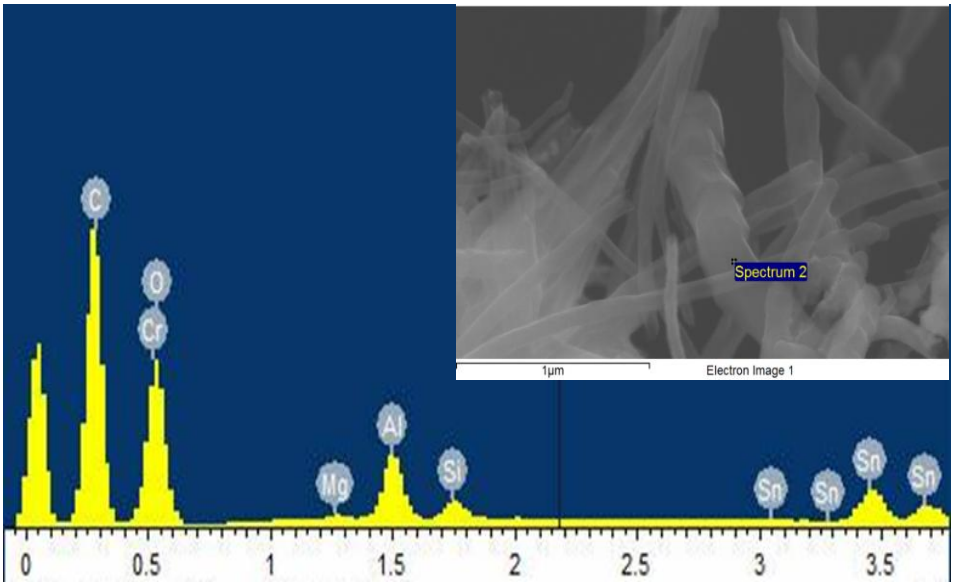

Figure 27: Representative EDS scan of chromium electroless plated CNTs. Inset shows the corresponding SEM image CNTs. Sn from sensitization step can also be seen. Other elements are from SEM sample holder.

To combat this problem, an electroless deposition of a Cr layer followed by an electroless deposition of a Cu-layer to protect the Cr layer was attempted. The results were similar to plating just Cr and showed that the oxidation of chromium likely occurred during the plating or washing step. The observed oxidation therefore cannot be easily prevented.

DISCUSSION OF RESULTS

The attempted mechanical incorporation of MWCNT by ball milling and extrusion failed to produce the desired microstructures. It appears that the clumps of MWCNTs are too tightly bound to be detangled or even broken by mechanical means. As a result, the NARloy-Z powders were covered with MWCNTs (Figures 5 & 6) and the consolidated material consistently showed MWCNTs on PPBs– see Figures 13 through 15 and 20. Lack of a uniform MWCNT distribution was believed to be the key underlying cause of the degradation of thermal conductivity in the NARloy-Z-MWCNT composite. The MWCNT clumps act as insulators since they are not in intimate contact with the matrix and cannot provide good transfer of thermal energy through the composite. This effectively reduced the cross sectional area and increased the tortuosity of the conduction path. As a result the thermal diffusivity and thermal conductivity decreased. The same argument applies to the increased electrical resistivity of the extruded composites.

Even with the MWCNTs on the powder surfaces, both FAST and extrusion achieved reasonably good consolidation of the composite powders. The consolidated material was bound together where NARloy-Z particles were able to weld together. The consolidated samples retained their shapes and could be easily handled. Table 3 shows that they even had a slightly higher yield strength than comparably processed NARloy-Z. If the MWCNTs can be better incorporated into the metal powders, it should be possible to achieve greater tensile strengths.

To eliminate the MWCNT incorporation and PPB segregation problems, it appears that the MWCNTs will have to be detangled and processed prior to milling as was done by Huang et al (Ref 5). This introduces an additional step and still may not be sufficient to fully disperse the volume fractions of MWCNTs desired to maximize the thermal conductivity of the composite. If a detangling step is done, it may be possible to apply a carbide forming element as a coating to the MWCNTs at the same time. This will allow using pure Cu in place of the NARloy-Z and still attain the desired interfacial properties. Based upon past experience, the welding phase for pure copper during ball milling persists much longer than that for NARloy-Z, so it should also be possible to work the MWCNTs into the powder better through longer milling times.

Another factor in the low thermal conductivities was the quality of MWCNTs used here. The MWCNTs were procured from Pyrograf Products, Inc. and were believed to possess high thermal conductivity. However, as was documented through testing at Vanderbilt University, the thermal conductivity of the MWCNTs were much lower than thought and generally much less than half the thermal conductivity of pure Cu rather than 10X higher as shown in Figure 22.

While Raman spectroscopy was selected as a way to screen the MWCNTs quickly, there are notable discrepancies between the D/G ratios and the measured thermal conductivities. The Sigma-Aldrich MWCNTs had the lowest D/G ratio at 0.09, but they had one of the lowest measured effective thermal conductivities. The contact resistances were not directly measured for this MWCNT, but they would have to be much greater than those measured for the CWRU sample to raise the intrinsic thermal conductivity above even 100 W/m-K. The CWRU MWCNTs, which did have the contact thermal resistances measured, show the highest thermal conductivity but also have a high D/G ratio at 0.47. The Pyrograf MWCNTs used for the composite work exhibited one of the lower D/G ratios at 0.26.

If one assumes that the contact thermal resistances are not similar in all tests, one can still use the D/G ratios to estimate the potential intrinsic thermal conductivity. If Pyrograf has about half the D/G ratio of CWRU, it should have about twice the thermal conductivity since it has half the defects. That would indicate a room temperature thermal conductivity on the order of 300 W/m-K. For the Sigma-Aldrich

sample the ratios would indicate that the thermal conductivity could be as high as 810 W/m-K. These values, while much better than the estimates based upon a constant contact thermal resistance, are still between about 1X and 2.7X the value of NARloy-Z. At best, a 10 volume percent addition would increase the MWCNT-NARloy-Z composite thermal conductivity 17%.

The oxidation of the Cr during plating represents a significant limitation of the wet chemistry method of coating the MWCNTs. Since it is unlikely that any wet chemistry method would prevent significant oxidation, other coating methods such as physical vapor deposition (PVD) including pulsed laser deposition may be required. The advantage of these techniques is that they occur in a high vacuum where oxidation of the Cr should be minimized. By changing from a Cr to a Cu target, the Cr can be protected by the application of a Cu layer. While this Cu layer will oxidize, the oxide is easily reduced later during FAST or other processing and should not be a significant problem. It may also be possible to deposit a sufficient amount of Cu on the Cr-coated MWCNTs to make the matrix. The blending process could be stopped, and the powder could be directly sintered using FAST.

The results with NARloy-Z-D composites, on the other hand, were very positive, with significant increases achieved in their thermal conductivity. The results are shown along with the results for Cu-D and Cu-Cr-D system in Figure 28 (Ref. 3). It is evident that thermal conductivity improvements were not observed in pure Cu-D system. The main difference between the composites was the presence of Zr in NARloy-Z, which forms ZrC at the Cu-D interface. Hence it is reasonable to conclude that ZrC lowered the contact thermal resistance of the Cu-D interface as predicted by the quantum mechanics-based model. Similar improvement was observed in Cu-Cr-Zr alloy (Figure 28) and in the Cu-Ti-D system where TiC at the Cu-D interface appears to lower the contact thermal resistance (Ref. 4). Therefore, it is recommended that further development of NARloy-Z-D and other diamond particulate reinforced copper-based composites be pursued for applications in rocket engine components.

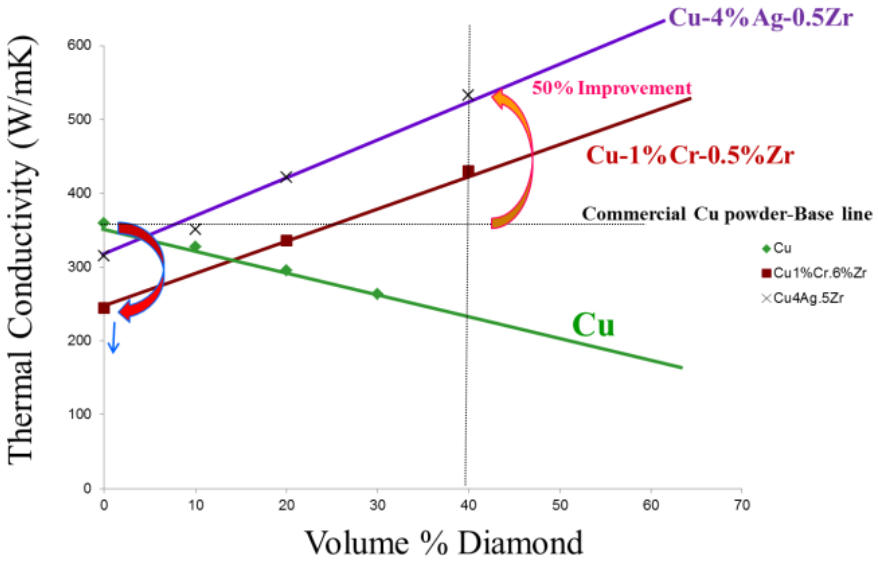

Figure 28: Thermal conductivity of copper-based alloy-diamond composites

It should be noted that the coating considerations discussed for MWCNTs apply equally to diamond powders. While agglomeration is not a problem for diamond powders they might benefit by coating with either carbide formers such as Zr or Cr and then over coated with copper to protect the coatings from oxidation.

SUMMARY, CONCLUSIONS AND RECOMMENDATIONS

NARloy-Z powder was blended with variable volume fractions of multiwall carbon nanotubes (MWCNTs) and Diamond (D) and sintered at an elevated temperature under pressure using FAST to produce fully dense NARloy-Z-MWCNT and NARloy-Z-D composites. Thermal conductivity of these composites was measured using the laser flash technique. NARloy-Z-D composites showed significant improvements in thermal conductivity as expected, but NARloy-Z-MWCNT composites showed a decrease in thermal conductivity. Microstructure analyses showed that Zr in NARloy-Z migrated to the carbon in both composites and provided the required low contact thermal resistance interface. The low thermal conductivity of NARloy-Z-MWCNT composites was attributed to a poor dispersion of MWCNT and the low thermal conductivity of the MWCNTs used. To improve the NARloy-Z-MWCNT thermal conductivity, several commercial MWCNTs were tested to find a commercial source that could provide high conductivity MWCNTs. However, this effort was not successful since all as-received MWCNTs had a low thermal conductivity.

For better MWCNT results, it is recommended to separate the MWCNTs and coat them with carbide forming metal such as Cr or Zr, followed by Cu or a Cu alloy for oxidation protection. The coatings also would help to keep the MWCNTs from forming clumps during blending. If enough Cu is deposited, it may also be used as the matrix, and the powders can be directly sintered using FAST.

NARloy-Z-D composites appear to be more promising in the short term. Their development should be pursued for applications in advanced rocket engines. Development of an optimized interface, diamond volume fraction and diamond particle size are the highest priority areas to pursue.

ACKNOWKEDGMENTS

This work was supported by NASA-STMD through the Center Innovation Fund (CIF). B. Bhat acknowledges the contributions of several MSFC Materials and Processes Laboratory personnel: Enrique Jackson (thermal diffusivity measurements), Dion Jones (SEM analysis) and Arthur Brown (XPS analysis). D. Li thanks Dr. Liming Dai's group at the Case Western Reserve University for providing MWCNT samples. TEM images of the Pyrograf MWCNTs and additional support were provided by Francisco Sola-Lopez of NASA GRC.

REFERENCES

1. A. Agarwal, S. R. Bakshi and D. Lahiri, "Carbon Nanotubes Reinforced Metal Matrix Composites", CRC Press, 2011.
2. K. T. Kim, J. Eckert, G. Liu, J. M. Park, B. K. Lim, and S. H. Hong, "Influence of embedded-carbon nanotubes on the thermal properties of copper matrix nanocomposites processed by molecular level mixing", Scripta Materialia, vol. 64 (2011), pp 181-184.
3. A. Rape, X. Liu, A. Kulkarni and J. Singh, "Alloy development for highly conductive thermal management materials using copper-diamond composites fabricated by field assisted sintering technology", Journal of Materials Science, February 2013, vol. 48, Issue 3, pp1262-1267.
4. B. Kieback, T. Weissgaerber, T. Schubert, and L. Rontzsch, "Nanostructured materials based on powder metallurgy route", presented at TMS 2013 Annual Meeting, San Antonio, TX, on March 5, 2013.
5. J.Y. Huang, Y.K. Wu and H.Q. Ye, "Ball Milling of Ductile Metals," Matls. Sci. and Eng. Vol. A199 (1995) pp. 165-172.
6. P.S. Gilman and J.S. Benjamin, "Mechanical Alloying," Ann. Rev. Mater. Sci., Vol. 13 (1983) pp. 279-300.
7. B.J. Kim, S.Y. Oh, H.S. Yun, J.H. Ki, C.J. Kim, S. Baik, and B.S. Lim, "Synthesis of Cu-CNT Nanocomposite Powder by Ball Milling," J. of Nanoscience and Nanotechnology, Vol. 9, No. 12, (Dec 2009) pp. 7393-7397.

8. L. Shi, D. Li, C. Yu, W. Jang, D. Kim, Z. Yao, P. Kim, and A. Majumdar, “Measuring Thermal and Thermoelectric Properties of One-Dimensional Nanostructures using A Microfabricated Device,” *J. Heat Transf.-Trans. ASME* **125**, 881-888 (2003).
9. D. Li, Y. Wu, P. Kim, L. Shi, P. Yang and A. Majumdar, “Thermal Conductivity of Individual Silicon Nanowires,” *Appl. Phys. Lett.* **83**, 2934-2936 (2003).
10. C. Yu, L. Shi, Z. Yao, D. Li and A. Majumdar, “Thermal Conductance and Thermopower of an Individual Single-Wall Carbon Nanotube,” *Nano Lett.* **5**, 1842-1846 (2005).
11. J. Yang, Y. Yang, S. W. Waltermire, X. Wu, H. Zhang, T. Gutu, Y. Jiang, Y. Chen, A. A. Zinn, R. Prasher, T. T. Xu and D. Li, “Enhanced and Switchable Nanoscale Thermal Conduction due to van der Waals Interfaces,” *Nature Nanotechnology* **7**,91-95 (2012).
12. J. Yang, Y. Yang, S. W. Waltermire, T. Gutu, A. A. Zinn, T. T. Xu, Y. Chen and D. Li, “Measurement of the Intrinsic Thermal Conductivity of a Multiwalled Carbon Nanotube and Its Contact Thermal Resistance with the Substrate,” *Small* **7**, 2334-2340 (2011).
13. M. Fujii, X. Zhang, H. Xie, H. Ago, K. Takahashi, T. Ikuta, H. Abe, and T. Shimizu, “Measuring the Thermal Conductivity of a Single Carbon Nanotube,” *Phys. Rev. Lett.* **95**, 065502 (2005).
14. A. Star, J. F. Stoddart, D. Steuerman, et al, “Preparation and properties of Polymer-Wrapped Single Walled Carbon Nanotubes”, *Angew. Chem. Int. Edn*. 2001, 40:1721- 1725.
15. K. Balasubramanian and M. Burghard, “Chemically Functionalized Carbon Nanotubes”, Small 2005, 1:180-192.
16. D. Tasis, N. Tagmaterchis, A. Bianco, et al, “Chemistry of Carbon Nanotubes”, Chem. Rev. 2006, 106:1105-1136.
17. Y. R. Wu, J. A. Philips, H. P. Liu, et al, “Carbon Nanotubes Protect DNA Strands during Cellular Delivery”, ACS Nano 2008, 2:2023-2028.
18. X. G. Hu, and S. J. Dong, “Metal Nanomaterials and Carbon Nanotubes—Synthesis, Functionalization and Potential Applications towards Electrochemistry”, J. Mater. Chem. 2008, 18:1279-1295.
19. F. Wang, S. Arai and M. Endo, “Metallization of Multi-walled Carbon Nanotubes with Copper by an Electroless Deposition Process”, Electrochem. Comm. 2004, 6:1042-1044.
20. H. Ago, T. Kugler, F. Cacialli, et al, “Work Functions and Surface Functional Groups of Multiwall Carbon Nanotubes”, J. Phys. Chem. B 1999, 103:8116-8121.
21. Y. Feng and H. Yuan, “Electroless Plating of Carbon Nanotubes with Silver”, J. Mater. Sci. 2004, 39:3241-3243.
22. Characterization of Carbon Nanotubes (CNTs) with Raman Spectroscopy, http://www.youngin.com/application/CNT.pdf
23. H. J. West, “Electrless Chromium”, Metal Finishing 1955, 53:62-63.
24. T. Ikumo, M. Katayama, M. Kishida, et al, “Metal-Coated Carbon Nanotube Tip for Scanning Tunneling Microscope”, Jpn. J. Appl. Phys 2004, 43:L644-L646.